ACS APPLIED MATERIALS & INTERFACES

Forum Article

www.acsami.org

DNA Molecular Beacon-Based Plastic Biochip: A Versatile and Sensitive Scanometric Detection Platform

Xiaoli Shi,[†] Jing Wen,[†] Yunchao Li,*[,†] Yue Zheng,[†] Jianjun Zhou,[†] Xiaohong Li,[†] and Hua-Zhong Yu*[,‡]

[†]Department of Chemistry, Beijing Normal University, Beijing 100875, P. R. China

[‡]Department of Chemistry, Simon Fraser University, Burnaby, British Columbia V5A1S6, Canada

Supporting Information

ABSTRACT: In this paper, we report a novel DNA molecular beacon (MB)-based plastic biochip platform for scanometric detection of a range of analytical targets. Hairpin DNA strands, which are dually modified with amino and biotin groups at their two ends are immobilized on a disposable plastic (polycarbonate) substrate as recognition element and gold nanoparticle-assisted silver-staining as signal reading protocol. Initially, the immobilized DNA probes are in their folded forms; upon target binding the hairpin secondary structure of the probe strand is "forced" open (i.e., converted to the unfolded state). Nanogold-streptavidin conjugates can then bind the terminal biotin groups and promote the deposition of rather large silver particles which can be either directly visualized or quantified with a standard flatbed scanner. We demonstrate that with properly designed probe sequences and optimized preparation conditions, a range of molecular targets, such as DNA strands, proteins (thrombin) and heavy metal ions (Hg^{2+}), can be detected with high sensitivity and excellent selectivity. The detection can be done in both standard physiological buffers and real world samples. This constitutes a platform technology for performing rapid, sensitive, cost-effective, and point-of-care (POC) chemical analysis and medical diagnosis.

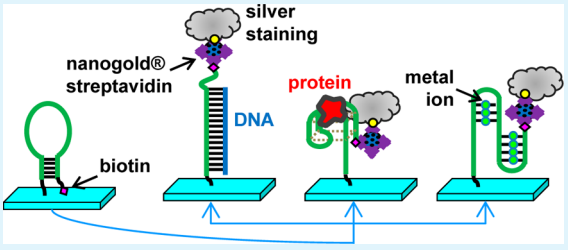

KEYWORDS: *plastic biochip, DNA molecular beacon, target-induced conformation switching, scanometric detection, medical diagnosis*

INTRODUCTION

The development of portable sensing devices for rapid, sensitive, and cost-effective point-of-care (POC) detection of targets of interest has long been sought because such devices are applicable for personal health care,[1−5] on-site environmental monitoring,[6−8] and rapid food toxins/bacteria screening.[9−12] However, it has been a challenging task to create a sensing platform having all the above-mentioned capabilities.[2−5,13−18] Colorimetric or scanometric biochips, in which each type of target can be captured by an appropriate probe immobilized at a specified location and inducing a color or darkness change, are promising candidates for fulfilling the requirements of cost-effectiveness, portability, and high detection throughput. They have attracted increasing attention in recent years, and have been developed for the detection of DNA,[14,18−20] protein/peptides,[5,13,21−26] and heavy metal ions.[16,27,28] However, the biochips developed previously either involve rather complex screening procedures or have limited sensitivity. Most of them run assays in a sandwich format (i.e., they employ immobilized probes to capture targets and then utilize reporters to transduce the biorecognition events), so that multiple-step surface reactions or additional labeling reagents are typically required. A simpler and more universal sensing strategy with a minimum number of reaction steps and of consumable reagents is needed for the development of commercial products.

A molecular beacon (MB)-based sensing strategy (i.e., target binding-induced conformational switching) is an alternative approach to the conventional sandwich-type bioassay and offers special advantages for rapid, sensitive, and label-free detection of target.[29−31] A molecular beacon typically refers to a single-stranded and dual-end fluorescently labeled oligonucleotide containing a stem-loop (hairpin-like structure). The short segments at its two ends are complementary, bringing the fluorophore and quencher into close proximity thus diminishing the fluorescence signals. Upon binding with complementary DNA strands, these structures are converted to rigid DNA duplexes (relocating the fluorophore farther away from the quencher), thus restoring the fluorescence signal.[29−31] In the past, MBs have been mainly employed as solution-based fluorescence sensors for the detection of DNA sequences,[29−35] though they were also immobilized on glass, gold and plastic substrates as surface-attached fluorescent probes for DNA target detections.[33−35] The detection principle of utilizing immobilized MB probes was typically based on the fluorescence quenching and recovering, which is similar to that developed recently on aptamer-graphene nanoconjugates.[36,37] In addition to applications in optical biosensors, MBs were adapted as surface-attached electrochemical probes by replacing their fluorophores with redox-active moieties.,[38−40] This common

Special Issue: Materials for Theranostics

Received: February 3, 2014
Accepted: May 14, 2014
Published: May 22, 2014

 © 2014 American Chemical Society

approach of binding-induced exposure of cryptic binding sties in biological systems has been further explored in the design of aptamer-based electrochemical biosensors for the enzymatically amplified detection of DNA.[41,42] Despite considerable progress over the past two decades, the MB-based technique is still limited to DNA-related research,[43−45] and it relies primarily on fluorescence or electrochemical reading methods.

In this paper, we report a novel molecular beacon-based plastic biochip platform for scanometric detection of various targets of interest. This type of biochip utilizes surface-immobilized hairpin-DNA strands which are dually modified with an amino group (for surface coupling) and a biotin group (for signal reporting via streptavidin-gold nanoparticle-assisted silver staining). The detection principle is as follows (Scheme 1): without the target, the immobilized hairpin probe strand, DNA molecular beacon (MB) is in a "closed" state, which brings the biotin group to the substrate surface (i.e., "buried" underneath the MB probe). In the presence of targets, the hairpin-like structure is forced to unfold (to an "open" state) by the binding event, which allows the nanogold-streptavidin conjugates to interact promptly with the biotin groups and produce a visual signal upon silver staining (the deposition of submicrometer size silver particles). As proof of concept, we have demonstrated that this type of plastic biochip is able to detect DNA strands, protein and heavy metal ions by integrating specially designed binding domains into the MB probe strands (Scheme 1). We believe that this is the first example of molecular beacon-based scanometric biochips that is able to sensitively detect a range of molecular analytes, augmenting its potential for performing POC analysis and diagnosis.

Scheme 1. Principle of DNA Molecular Beacon (MB)-Based Plastic Biochips for Scanometric Detection of Various Targets (DNA, Protein, or Metal Ion)

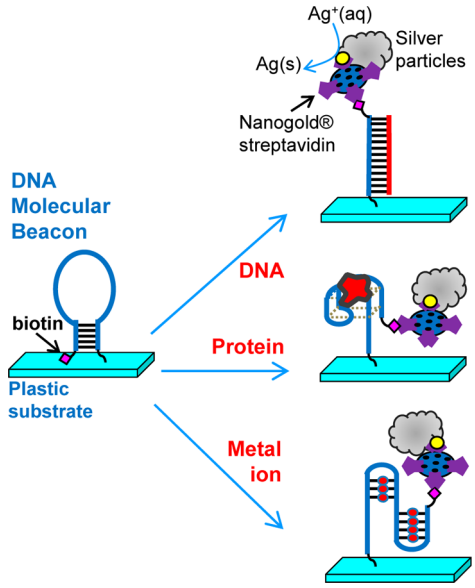

EXPERIMENTAL SECTION

Reagents. All chemicals were of analytical grade and used as-received. Sodium citrate, citric acid, sodium dihydrogen phosphate (NaH_2PO_4), magnesium chloride, sodium chloride, mercuric nitrate, hydrochloric acid, and disodium hydrogen phosphate (Na_2HPO_4) were purchased from Beijing Chemical Reagent Co. (Beijing, China). Tris(hydroxy-methyl)-aminomethane hydrochloride (Tris - HCl), silver acetate, hydroquinone, thrombin from human plasma, 1-ethyl-3-(3′-dimethylaminopro pyl) - carbodiimide (EDC), *N*-hydroxy-succinimide (NHS), bovine serum albumin (BSA, globulin- free, molecular biology grade), Tween 20, glycerol, gelatin and sodium azide, were ordered from Sigma-Aldrich (Saint Louis, MO, USA). Human plasma IgG was purchased from KPL Inc. (California, USA). Modified and unmodified oligonucleotides (sequences are listed in Table 1) were of HPLC-purification grade and obtained from Shanghai Sangon Biotechnology Inc. (Shanghai, China). Nanogold-streptavidin conjugates were ordered from Nanoprobes Inc. (New York, USA). Deionized water to prepare all the solutions was produced from a Barnstead Easypure System (Thermo Scientific Inc., Dubuque, Iowa, USA). Human serum, blood plasma, and whole blood (from a healthy people) were provided by the Affiliated Hospital of Beijing Normal University. The lake and industrial wastewater samples were taken from Kunming Lake in Beijing and an electroplating factory in Shenyang, respectively. PC substrates were obtained from regular CDs (or CD-Rs) by removing the reflective metal layer and the dye layer.

Table 1. Oligonucleotide Sequences of Molecular Beacon Probes and Target DNA Strands

DNA strand		sequence
DNA MB probes	ST-5	5′ -biotin-CGAGGTAAAACGACGGCCAGTCCTCG-$(CH_2)_6$-NH_2-3′
	ST-6/SP-C6	5′ -biotin-GCGAGGTAAAACGACGGCCAGTCCTCGC-$(CH_2)_6$-NH_2-3′
	ST-7	5′ -biotin-GGCGAGGTAAAACGACGGCCAGTCCTCGCC-$(CH_2)_6$-NH_2-3′
	ST-5(FL)	5′ -TAMRE-CGAGGTAAAACGACGGCCAGTCCTCG-Dabcyl-3′
	ST-6(FL)	5′-TAMRE-GCGAGGTAAAACGACGGCCAGTCCTCGC-Dabcyl-3′
	ST-7(FL)	5′ -TAMRE-GGCGAGGTAAAACGACGGCCAGTCCTCGCC-Dabcyl-3′
	SP-C9	5′ -biotin-spacer9-GCGAGGTAAAACGACGGCCAGTCCTCGC-$(CH_2)_6$-NH_2-3′
	SP-C18	5′ -biotin-spacer18-GCGAGGTAAAACGACGGCCAGTCCTCGC-$(CH_2)_6$-NH_2-3′
DNA targets	PM	5′ -GACTGGCCGTCGTTTTACC-3′
	1-NP	5′ -GACTGGCCGACGTTTTACC-3′
	2-NP	5′ -GACTGGCCTACGTTTTACC-3′
	NP	5′ -TCACCAGTTCGCCACGCAA-3′
MB probes for protein (thrombin)	TBA-5	5′ -NH_2-$(CH_2)_6$-TTT CCA ACT TGG TTG GTG TGG TTG GTC T-biotin −3′
	TBA-6	5′-NH_2-$(CH_2)_6$-TTT CCA ACT TGG TTG GTG TGG TTG GAC T -biotin −3′
	TBA-7	5′ -NH_2-$(CH_2)_6$-TTT CCA ACT TGG TTG GTG TGG TTG GAA T-biotin-3′
MB probes for metal ion (Hg^{2+})	T-T probe 1	5′-NH_2-$(CH_2)_6$-AC AAA GAC TTT GTT CCC CTT CTT TGA -biotin-3′
	T-T probe 2	5′ -NH_2-$(CH_2)_6$-AC AAA GAAC TTT GTT CCC CTT CTT TGA -biotin −3′
	T-T probe 3	5′-NH_2-$(CH_2)_6$-CAAAGG A ACT TTG GTT TC CCTT TTC CTT TT-biotin-3′

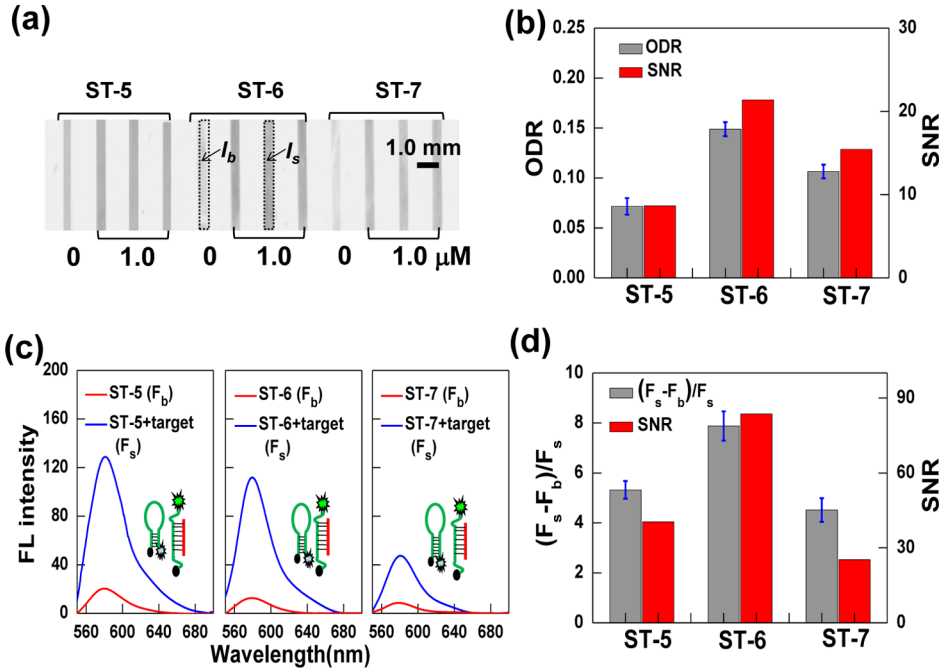

Figure 1. Effect of stem length on the performance of DNA MB-based plastic biochips. (a) Representative optical image of the DNA MB biochip designed with different stem lengths (5 bp, ST-5; 6 bp, ST-6; 7 bp, ST-7). For each system, a blank (without the DNA target strand) and three replicates of the sample lines (1.0 M DNA PM target) were tested simultaneously. The concentration of the DNA MB probes to prepare these chips was 10 μM for all cases, and the sliver staining time was kept at 18 min; (b) correlation between the assay signal (ODR) and signal-to-noise ratio (SNR) with the stem length; (c) Representative fluorescence spectra of the DNA MB probes (0.5 μM) containing different lengths of stem respond to blank (red line) and target (1.0 μM, blue line) in solution. (d) Correlation between stem length and binding signal (FL intensity) and SNR of the solution-diffused DNA MB probes in response to the added target DNA(1.0 μM). The experimental uncertainties (error bars) shown in shown in b and d were obtained from the parallel chip results (panel a and Figure S1 and Figure S2 in the Supporting Information). The insets in c are the hypothetic conformations of the DNA MB probes before and after target binding.

Instrumentation and Surface Characterization. The plastic substrates were activated in a UV/ozone cleaner (Model PSD-UV, Novascan Technologies Inc.). A JASCO J-810 spectropolarimeter was utilized to collect CD spectra, a UV-2450 UV−vis spectrophotometer (Shimadzu Co.) was used to record the absorption spectra, and a PerkinElmer-LS55 fluorescence spectrometer (USA) was employed to collect the fluorescence spectra. The flatbed scanner for obtaining optical images of the plastic biochips was from Microtek (Scanmaker i700), which can be operated in either transmission or reflection mode. The surface topographies of the binding stripes or dots were imaged with an atomic force microscope (Asylum Research, Inc.) in tapping mode.

Surface Activation of PC Substrates. PC plates were first sonicated in ethanol for 10 min and then illuminated in a UV/ozone system for 15−30 min. The substrates were subsequently immersed in a 0.1 M phosphate buffer at pH 6.0 containing 5 mM EDC and 0.3 mM NHS for 3−5 h to activate the surface-tethered carboxylic acid groups, followed by rinsing with PBS buffer (containing 20 mM phosphate, 150 mM NaCl, pH 7.4), and drying in a stream of nitrogen gas.

Fabrication of DNA MB-Based Biochips. The optimal DNA MB probes (their sequences are listed in Table 1) were diluted to 5.0−20 μM by using 10 mM Tris coupling buffer (also containing 0−150 mM NaCl, 50 mM $MgCl_2$, pH 7.4), and then delivered onto the PC surface through a PDMS (polydimethylsiloxane) stamp. It was prepared against a silicon master, and has 14 embedded microchannels (each channel of 500 μm width and 2.5 cm length). The flow rate of the samples in the channels was kept in the range of 10−30 μL/min. The PC sheet was then kept in a humid box for 4−10 h to form the probe line arrays. The substrate was rinsed thoroughly with 10 mM Tris buffer and soaked in a blocking buffer (20 mM phosphate, 150 mM NaCl, 3% BSA, pH 7.4) for 1−3 h to passivate the substrates. After washing, various targets (DNA, thrombin, and Hg^{2+} ions) in buffers or in real world samples were introduced into the channels and kept for 60 min. Afterward, the PDMS plate was peeled off and the plastic chip was washed with PBS buffer. Finally, the biochip was immersed in a solution containing nanogold streptavidin conjugates for 30−60 min and subjected to silver staining. Before staining, the plastic biochips need to be washed thoroughly with deionized water to remove interfering anions. They were then immersed in a freshly made silver enhancement solution consisting of silver salt (12 mM silver acetate) and reducing agent (45 mM hydroquinone) for 10−20 min. It is noteworthy that the silver enhancement solution (after mixing) must be replaced with a fresh solution every 10 min in order to obtain satisfactory results.

Signal Readout and Data Analysis. After sliver staining, the plastic biochips were imaged with the Microtek flatbed scanner in the transmission mode; this also can be done with standard office scanners in the typical reflection mode. The images were scanned as color pictures at 600 dpi, and were subsequently converted to grayscale images using Adobe Photoshop (version 10). The average luminosity (I_s) of each binding stripe was measured using the histogram tool in Adobe Photoshop and normalized by the background luminosity (I_b) (from the assay stripe corresponding to the blank experiment (i.e., [target] = 0) to determine its optical darkness ratio (ODR)

$$\mathrm{ODR} = \frac{I_b - I_s}{I_b} \quad (1)$$

For a better comparison, the signal-to-noise ratio (SNR or S/N) of each binding stripe was also calculated by using the following equation:[46]

$$\mathrm{SNR} = \frac{\text{mean}}{\text{standard deviation}} = \frac{\overline{\mathrm{ODR}}}{s_{\mathrm{ODR}}} \quad (2)$$

where $\overline{\mathrm{ODR}}$ and s_{ODR} are the mean and standard deviation of ODR values. To obtain these values, at least three replicates (three parallel

dx.doi.org/10.1021/am5007029 | ACS Appl. Mater. Interfaces 2014, 6, 21788−21797

chips or three replicated stripes on the same chip) were prepared and measured.

RESULTS AND DISCUSSION

To construct MB-based plastic DNA biochips, we adopted surface-immobilized hairpin-DNA strands as recognition elements and gold nanoparticle-assisted silver staining as signal enhancement method. For scanometric detection of various molecular targets, two requirements must be met: low background signal (i.e., high selectivity) and high response signal in the presence of target (i.e., high sensitivity). As an example, we will first take an MB-based plastic biochip designed for detecting a sequence-specific DNA target, to illustrate how the stem length, linker length, and assembly condition (probe concentration, salt concentration, and blocking condition) affect the background and response signals.

Effect of the Stem Length. The stem length is a key parameter that determines the response of a DNA MB to its target:[33,44−46] if the stem is too long (more than eight base pairs), the MB prefers to form a stable hairpin-like conformation which is difficult to open, showing a low background and a low response signal. If the stem is too short (less than five base pairs), the hairpin-like conformation of the MB is easy to open, and exhibits a high background signal and a high response signal simultaneously. Hence the stem length of the MB must be properly chosen in order to obtain a good balance between high response signal (i.e., high sensitivity) and low background signal (i.e., high selectivity). According to previous studies, a DNA MB containing a 15−35 bp loop typically needs a 5−7-bp stem to stabilize its stem-loop conformation.[33,47−49]

To determine the optimal stem length, we immobilized three DNA MB probes (Table 1) that contain the same loop (16 bp) but different stem lengths (5−7 bp) on the same chip as line arrays and examined their responses to the same concentration of complementary DNA targets (1.0 μM, three repeats plus a blank). We note that multiple samples (at least three independent chips for each experiment) have been prepared and tested under identical conditions (concentrations of both probe and target DNA as well as buffer solutions) to validate the reproducibility and to obtain statistic results (see Supporting Information). Figure 1(a) shows a representative chip image of three MB-based detection systems with different stem length. It is clear that the triplicate binding stripes in the presence of the DNA target (1.0 μM, sequence shown in Table 1) are distinct (darker) from the blank (0 μM) and are uniform across the three replicates. The darkness of the blank stripes are also different from each other, which shows a decreasing trend on the order of 5 bp > 6 bp > 7 bp.

The binding assays were quantified by the optical densitometry analysis technique as described previously.[54] As illustrated in Figure 1a, the average luminosity (I_s) of each binding stripe was measured using the histogram tool in Photoshop, and the background luminosity (I_b) was determined by selecting the assay stripe corresponding to the blank experiment (0 μM). The optical darkness ratio (ODR) of each assay stripe was then calculated using eq 1.[54] In Figure 1b, we have shown that the three surface-tethered MBs produced distinct responses in terms of the determined ODR values, and, the one with a 6-bp stem (**ST-6**) shows the best detection performance. For a better comparison, we have also calculated the signal-to-noise ratio (SNR or S/N) based on eq 2 for each system. It is important to notice in Figure 1b that the SNR values shows the same trend as that for signal change, i.e., the ST-6 has the highest value in all three variants.

To confirm the above observation, we also employed fluorescence spectroscopy to examine the three MB probes with different stem lengths in solution. As shown in panels c and d in Figure 1, the responses of the three MB probes in solution are quite similar to those of their counterparts on the surface: the MB with a 6-bp stem shows the best detection performance. Therefore, we chose a 6-bp stem (ST-6) for a DNA MB containing a loop of ca. 20 nucleotides for the following tests. However, if the target is not a sequence-specific DNA, the stem length of the probe may need further optimization because the interaction between the probe and the target in that case is not the same as for complementary DNA strands.

Effect of the Label Attachment. The length of the linker between the biotin group and the terminus of a DNA MB probe is another key parameter, as it directly relates to the steric effect of the biotin residues in the "closed" and the accessibility of such groups in the "open" conformation.[33,47,48] To determine the optimal linker length, we compared the previously used C6-linker (SP-C6) with two longer versions (SP-C9, SP-C18) (Table 1). As shown in Figure 2, three types

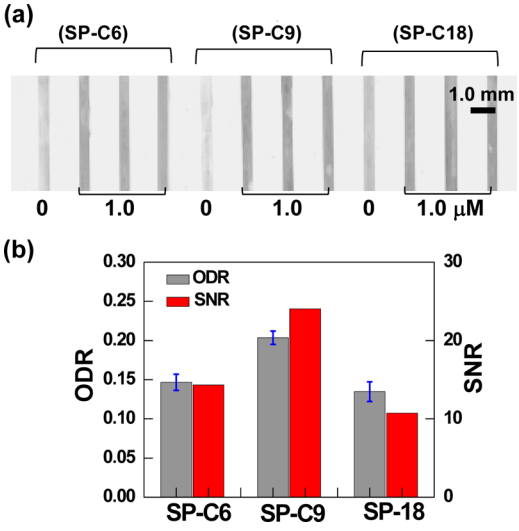

Figure 2. Effect of the label linker of DNA MB probes on the background and response signals. (a) Representative optical image showing the line array of the surface-immobilized DNA MB probes (10 μM ST-6) containing different label linkers (SP-C6, SP-C9, and SP-C18) with/without binding the DNA target (1.0 μM PM target) and undergone 18 min silver staining treatment, (b) signal level (ODR value) and signal-to-noise ratio (SNR) of the surface-immobilized DNA MB probes shown in a. The experimental uncertainties (error bars) shown in b were obtained from the parallel assay lanes shown in a.

of surface-tethered MBs that have the same sequences but different linker lengths (for the biotin attachment) produced different signal responses (different ODR values). The MB of the most extended spacer (SP-C18) generated the highest blank signal and the highest response signal while the one of the medium length (SP-C9) gave the highest signal-to-noise ratio (SNR). We speculate that the MB of a SP-C9 biotin linker may have the most suitable length to allow biotin to be in close proximity to the substrate in its "closed" state, and to allow the

dx.doi.org/10.1021/am5007029 | ACS Appl. Mater. Interfaces 2014, 6, 21788−21797

reporter (i.e., nanogold streptavidin conjugates) to easily approach the biotin groups in the "open" state.

Effect of the Assembly Conditions. Besides the probe structure, its immobilization condition such as probe concentration, salt concentration and blocking reagents can also exert a significant influence on the background (blank) and response signals as these parameters can affect the probe surface density, stability and steric effect for target binding.[20,47,48,50,51] To examine the influence of the probe concentration, we created ten MB probe lines (two lines for each concentration) on the same plastic chip by using different concentrations of probe solutions (from 2.0 μM to 50 μM). As shown in Figure 3(a), the background signal and the response signal both increase considerably at the beginning and then reach saturation at high concentrations. However, the line formed with the 10 μM probe shows the highest signal-to-noise ratio. It is expected that an increased probe surface density will lead to an enhanced signal response but the background signal is also rising. This phenomenon may be due to the fact that more MB probes cannot form hairpin-like conformations at increased probe surface density. Therefore, the probe lines formed with a medium concentration (10 μM), may provide the most favorable environment to create probe arrays with optimized surface density and conformation. It should be noted that such optimal DNA probe concentration is 2.4−5.0 times lower than that used for attaching linear DNA probes (typically 25−50 μM) on the same PC surfaces, indicating that the MB probes require much larger space to unfold upon immobilization.

The effect of salt (especially Mg^{2+}) concentration in the assembly buffer was analyzed by using a series of 10-μM SP-C9 solutions containing different concentrations of Mg^{2+} (0, 25, 50, 100, 200 mM) to construct probe lines on the substrates. As shown in Figures 3b, the effect of the Mg^{2+} concentration on the background signal and on the response signal is similar to that of the probe concentration, i.e., both increase gradually and reach saturation when the Mg^{2+} concentration in the assembly buffer increases. The probe lines formed at 50 mM [Mg^{2+}] have the highest signal-to-noise ratio. This interesting phenomenon can be understood by considering the two roles that Mg^{2+} ions play in the above bioassays: they not only enhance the density of surface-bound probes but also stabilize the DNA structures by reducing the intra- and intermolecular repulsive forces of DNA strands. Therefore, a buffer with moderate concentrations of Mg^{2+} (25−50 mM) should offer the most favorable environment to create probe arrays with optimized surface density and conformation.

It is imperative to block (passivate) the substrates after immobilizing DNA probes in order to enhance the overall chip performance.[14,20] The blocking step typically has the following functions: blocking the entire substrate surface to reduce nonspecific absorption, passivating the remaining carboxyl groups, and embedding the biotin groups in hairpin structures to avoid side reactions. The blocking effect mainly depends on substrate affinity, molecular size and concentration of the blocker. To find an optimal blocking condition, first we tested macromolecular blockers (BSA, glycogen, and skim milk powder), small molecular blockers (T10 and lysine) and mixed reagents (BSA and glycogen). As shown in Figure 3c, BSA exhibits the best blocking effect. It has a strong affinity to the substrates with activated carboxyl groups, and imposes a significant steric effect for binding nanogold streptavidin conjugates. Analysis of the results revealed that a 3% BSA

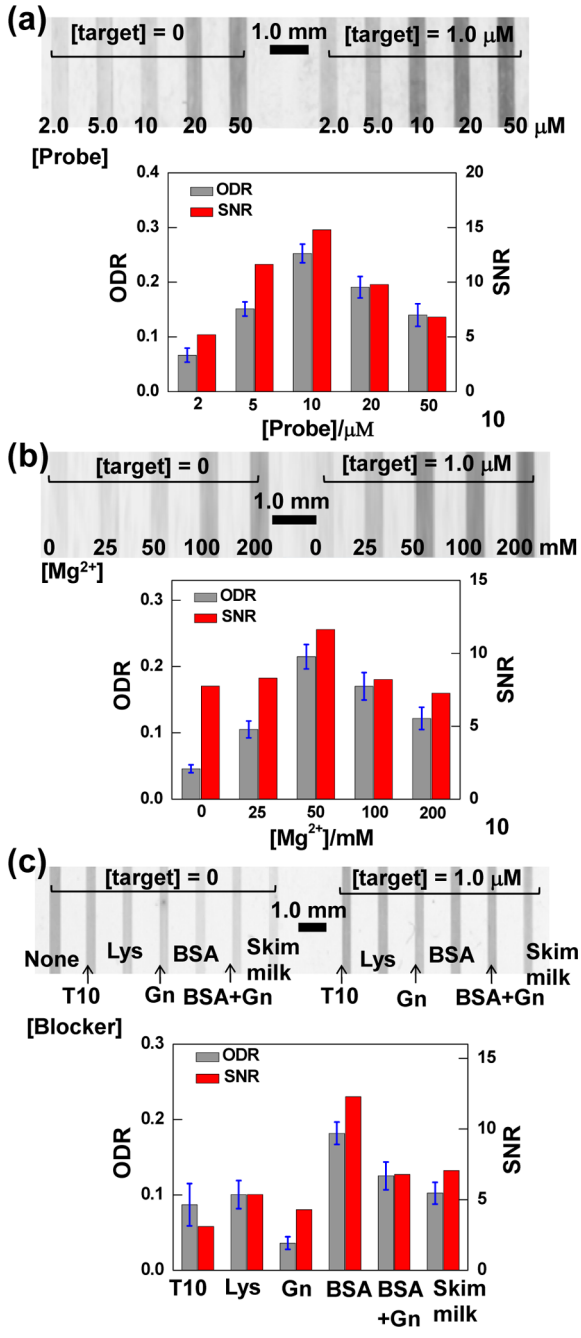

Figure 3. Effect of the probe assembly conditions on background and response signals. (a) Representative optical image showing the responses of the probe arrays created at various probe concentrations (SP-C9) and dependence of ODR and SNR on the probe concentration, (b) a representative optical image showing the responses of the probe arrays created with solutions containing 10 μM MB probe (SP-C9) and different concentrations of Mg^{2+}, and dependence of ODR and SNR on Mg^{2+} concentration in the coating buffer (20 mM Tris +150 mM NaCl, pH 7.4), (c) representative optical image showing the responses of the probe array created by using a coating buffer containing 10 μM SP-C9 probe plus 50 mM Mg^{2+} but different types of blocking reagents, and dependence of ODR and SNR on the type of blocking reagents. The staining time for the chips in a−c was kept at 20 min in all cases. The experimental uncertainties (error bars) were obtained from the replicated, independently fabricated chips (see Figure S3 in the Supporting Information).

dx.doi.org/10.1021/am5007029 | ACS Appl. Mater. Interfaces 2014, 6, 21788−21797

solution yields the highest signal-to-noise ratio (see Figure S4 in the Supporting Information).

We are now able to formulate an optimal protocol for the design and immobilization of DNA MB probes on plastic substrates, which allows us to construct and implement MB-based biochips for POC analysis and diagnostics. As proof of concept, we tested this new type of biochips for the detection of a representative set of analytical targets, DNA strands, protein (thrombin), and heavy metal ions (Hg^{2+}).

Detection of DNA Targets. Rapid, simple, and sensitive detection of sequence-specific DNA strands has attracted much attention owing to its importance in gene profiling, antibioterrorism, and forensic applications.[52,53]Therefore, we first tested the MB-based DNA biochips for the detection of complementary DNA strands (PM target). As shown in Figure 4, upon binding with different concentrations of target DNA,

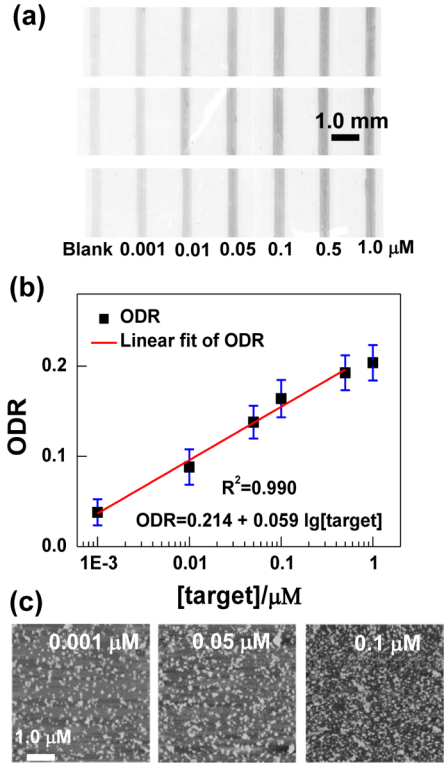

Figure 4. Plastic DNA MB biochips for scanometric detection of complementary DNA targets. (a) Three representative chip images showing the responses of surface-immobilized DNA MB probes (formed with 10 μM SP-C9 probe) to different concentrations of target DNA strands (PM target) (with 15 min silver staining), (b) dependence of the ODR on target concentration. The experimental uncertainties were derived from the replicated chip results shown in (a); the red line is the linear fit to the experimental data, R^2 = 0.990, (c) representative AFM images to show the size and density of silver/gold nanoparticles within the binding stripes.

the probe lines on all three representative chips are visible to naked eyes with 10−20 min silver staining; their ODR values were found to increase monotonically with increased target concentration (the higher the concentration, the darker the binding stripe). Further analysis revealed that the biochips have a linear dynamic range from 1.0 nM to 0.5 μM and are able to detect as little as 1.0 nM or 1.0 fmol (as only 1.0 μL needed) target DNA. Such a detection limit is about ten times better than that of biochips with sandwich-assay architecture,[18] demonstrating the advantage of using DNA molecular beacon as the sensing component. It should be pointed out that the linear dynamic range of the biochips can be widened by tuning the silver staining time.[18,54]

As shown in Figure 4c, atomic force microscopy (AFM) images revealed that the binding stripes are composed of large-size silver nanoparticles (ca. 40−150 nm, depending on staining time and the density of gold nanoparticles initially bounded, see Figure S5 in the Supporting Information); particle densities gradually increase with increasing DNA target concentration. The correlation between the particle density and the target concentration constitutes a direct proof for target-binding-induced conformational changes of the MB probes on the surface. Although the particle density was observed to be proportional to the ODR value of the binding sites, the relationship between them is rather complicated because of the ODR value being a function of both particle size and distribution.[54]

To evaluate the selectivity of this MB-based biochip for detecting DNA strands, we challenged the biochip with single-base mismatched targets (1-NP), two-base mismatched targets (2-NP), and noncomplementary targets (NP) (sequences are listed in Table 1). As shown in Figure 5, the response of the

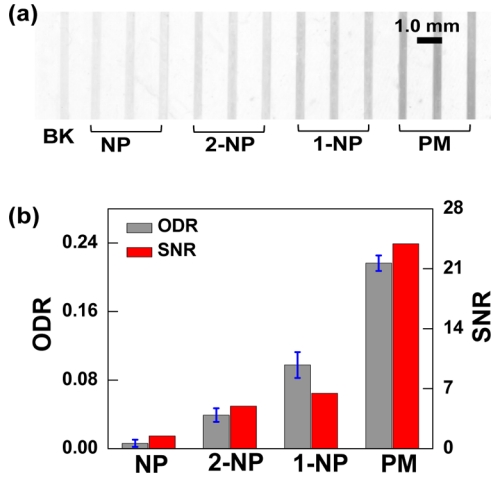

Figure 5. . DNA MB-based plastic biochips for discriminating base-pair mismatches. (a) Representative optical image showing the responses of surface-immobilized MB probes (formed with 10 μM SP-C9) to 1.0 μM DNA targets containing different numbers of base-pair mismatches (PM, perfect match; 1-NP, one-base mismatch; 2-NP, two-base mismatch; NP, noncomplementary; BK, blank) (with 15 min silver staining), (b) dependence of the ODR and SNR on the number of base mismatches in DNA targets. The experimental uncertainties (error bars) shown in b were determined from the three repeating binding stripes shown in a.

probe lines upon incubation with the above strands are visually different: the ODR values of the signal lines corresponding to 1-NP, 2-NP and NP account for 45, 18, and 3% of those corresponding to PM (prefect match target). The change in the SNR values shows a very similar trend as that of ODR. These results confirm that this MB-based biochip is capable of differentiating a single-base mismatch in a sequence-specific DNA target.

Detection of Thrombin. As a serine protease, thrombin plays a crucial role in blood coagulation cascade, thrombosis, and hemostasis.[55] Thus, detection and quantitation of this protein is of particular medical importance.[21,56−58] Here we

demonstrate the application of an MB-based biochip for thrombin detection, adapting a specially designed MB probe containing a thrombin-binding aptamer (TBA-6).[57,58] The sequence of the TBA probe was optimized (see Figure S6 in Supporting Information) and is listed in Table 1.

UV−vis absorption spectroscopy and circular dichroism (CD) spectroscopy were first carried out to confirm the binding between TBA-6 probe and thrombin in solution as well as the binding-induced conformational switching (see Figure S7 in the Supporting Information). The chip-based assays were then performed. This biochip exhibits a good response to different concentrations of thrombin (from 10 nM to 5.0 μM), evidenced by the signal lines with different optical darkness (see Figure S8 in the Supporting Information). It shows that this chip can detect as little as 10.0 nM or 10.0 fmol (1.0 μL × 10.0 nM) thrombin in buffer solution. Because the concentration of thrombin in blood can increase to nM or even low μM level at disease conditions,[59,60] this biochip meets the general requirement for such thrombin quantification. Moreover, this biochip demonstrates a good selectivity to thrombin as it did not show discernible responses to other more abundant proteins in serum (see Figure S9 in the Supporting Information). In consideration of "real life" applications, we further challenged this biochip with human serum, blood plasma and whole blood samples (i.e., diluting thrombin with these biological fluids to various concentrations), respectively. As shown in Figure 6, the response of the biochip to the thrombin in human serum is found as impressive as that in buffer solution, and the limit of detection (LOD) was determined to be 10 nM. As for the thrombin present in blood plasma or whole blood, this biochip still responds quantitatively, although the signal in both cases are not as strong as that in human serum (especially for the whole blood, see Figure S10 in the Supporting Information).

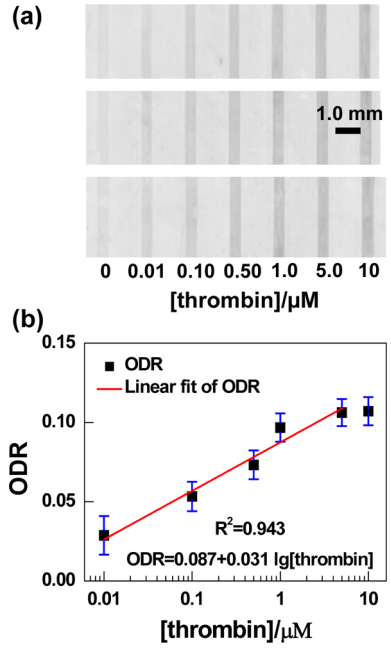

Figure 6. Plastic MB-based biochips for scanometric detection of thrombin. (a) Representative chip images showing the response of surface-immobilized DNA MB probes (formed with 10 μM TBA-6) to different concentrations of thrombin in human serum (15 min silver staining), (b) dependence of ODR on thrombin concentration in human serum (the solid line is the linear fit of the experimental data, R^2 = 0.943. The experimental uncertainties (error bars) shown in shown in b were obtained from the replicated chip results shown in a.

Detection of Hg^{2+}. Mercury ion, a widespread highly toxic contaminant in aquatic ecosystems, poses severe adverse effects on human health and the ecosystem.[61,62] Rapid on-site and sensitive detection of Hg^{2+} in aqueous media is of great importance.[16,27,63−65] To further demonstrate the versatile applications of MB-based DNA biochips, we have designed a DNA MB probe containing thymine (T)-rich fragments (T-T probe in Table 1)[62,63] which utilizes T-Hg^{2+}-T coordination-induced conformational switching for the detection of Hg^{2+}. In this design, the conformation of the T-T rich probe is expected to convert from a hairpin-like to an "S-like" structure upon binding Hg^{2+} (Scheme 1); the probe sequence was optimized prior to the sensitivity and selectivity tests (see Figure S11 in the Supporting Information).

In order to test the feasibility of the above design, absorption spectroscopy and CD spectroscopy were employed again to confirm the interaction between T-T probe and Hg^{2+} ions in solution (see Figure S12 in the Supporting Information). Then chip-based assays were carried out to assess the response of this MB-based biochip to Hg^{2+}. As shown in Figure 7, the biochip has demonstrated excellent performance: we were able to quantitate Hg^{2+} in the concentration range from 5.0 nM to 50 μM. The detection limit achieved here is as low as 5.0 nM (1.0 μL × 5.0 nM = 5.0 fmol) in lake water. Such a value is about half of the maximum contaminate level (MCL) of mercury in drinking water recommended by the World Health Organization (WHO),[66] indicating that this biochip has the capability to evaluate Hg^{2+} contamination in common drinking water. In fact, the response of this biochip to Hg^{2+} in tap water is excellent (see Figure S14 in the Supporting Information).

In considering the complexity in practical applications, we further challenged this biochip with a wastewater sample from an electroplating factory containing unknown concentration of Hg^{2+}. Upon determining the Hg^{2+} concentration in the sample by ICP atomic emission spectroscopy (AES), we compared the responses of our chip to the industrial waste, lake, and tap water samples. The latter two were spiked with the same concentration of Hg^{2+} (5.5 μM) for direct comparison. We discovered that the biochip displayed similar signal responses to all three samples (see Figure S15 in the Supporting Information), augmenting its potential in performing real world water analysis. Moreover, we confirmed that this Hg^{2+}-sensing biochip has a low cross-talk with most cations in solution (including Mg^{2+}, Ca^{2+}, Cu^{2+}, Zn^{2+}, Ba^{2+}, Mn^{2+}, Co^{2+}, Cd^{2+}, Ni^{2+}, Al^{3+}, Fe^{3+}, and Li^{+}, demonstrating its excellent selectivity (Figure 7c, d).

General Performance and Comparison with Other Methods. As a new addition to the scanometric detection family, we need to discuss the measurement reproducibility (precision), quantitation accuracy by comparing our chip results with other well established analytical protocols. According to replicated experiments (Figures 1−6 and Table S1 and S2 in the Supporting Information), the relatively standard deviation (RSD), 1/SNR of the signal among the parallel stripes on the same chip and among the stripes on independent chips were found to be around 5.0 and 10%, respectively, indicating this biochip having a good reproducibility as long as the assay conditions were kept identical. Because this biochip displays a quantitative response to the three kinds of targets over a large concentration range (Figures 4, 6, and 7), we should be able to quantify these targets based

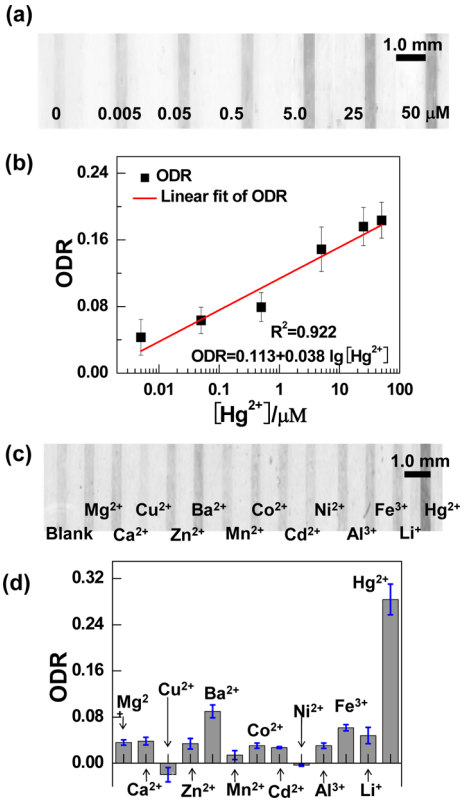

Figure 7. Plastic MB-based biochips for scanometric detection of Hg^{2+}. (a) Representative optical image showing the responses of surface-immobilized DNA MB probes (formed with 10 μM T-T probe) to different concentrations of Hg^{2+} in lake water (20 min silver staining), (b) ODR as a function of the Hg^{2+} concentration (the red line is the best linear fit to the experimental data, R^2 = 0.922), (c) representative optical image showing the responses of surface-immobilized DNA MB probes to different metal cations of 1.0 μM in all cases, (d) ODR of the biochip corresponding to different metal cations (1.0 μM). The experimental uncertainties (error bars) shown in b and d were obtained from the replicated, independently fabricated chips (the original images of these replicates are included in the Supporting Information as Figure S13).

on these calibration curves (the linear fits). Certainly, the quantitation assays should be performed under the conditions exactly the same as that used for the construction of the calibration curves. In addition, the calibration curves with more data points should be obtained in order to achieve the optimized quantitation accuracy.

After each use, the plastic MB-based biochips can be regenerated by treating first with a "back-developed" solution (containing $Na_2S_2O_3$ and $K_3Fe(CN)_6$) to remove the silver particles, and then with hot water (~80 °C) to dissociate the binding assays completely. Although the regeneration treatment is quite harsh, the response of the regenerated biochip was found to decrease only ~15% after three rounds of tests (see Figure S16 in the Supporting Information), indicative of its satisfactory regeneration performance. In addition, we have assessed the biochip stability by storing it for different periods of time; it was observed that the aged biochip can still produce a response accounted for ca. 80% of the original signal after 2 weeks (see Figure S17 in the Supporting Information).

As we mentioned above, this type of biochip consists of a small plastic sheet (only costs several US cents) and a tiny amount of DNA oligomers (with regular modifications and no fluorescent or redox labeling); the consumables are common reagents (gold nanoparticles, silver salts, etc.). The signal readout can be based on a standard office-use flatbed scanner (less than $100) for quantitative measurements or even naked eyes for qualitative determination. Therefore, compared with conventional fluorescence or electrochemical methods, this biochip platform shows the special advantages in cost-effectiveness and portability. It is noteworthy to mention that this biochip typically needs 30−60 min to get the results (because of the prolonged signal enhancement steps), which is longer than the time required for the fluorescence or electrochemical measurements. However, with optimized silver staining conditions (the concentration and type of the silver salts and reducing reagents), this can be eventually shortened (less than 10 min).

CONCLUSION

To meet the needs for developing portable analytical devices, we have designed a novel molecular beacon (MB)-based plastic biochip for scanometric detection of various targets of interest. The new plastic biochips adopt dually modified hairpin DNA strands containing target-binding domains as the recognition elements and utilize a binding-induced conformational switching (promoting silver deposition) signal generation protocol. To achieve satisfactory performance, we have systematically investigated and optimized the molecular structure, as well as assembly and application conditions. We were able to construct and implement such biochips for POC analysis of three types of popular analytes: DNA targets (down to 1.0 nM), protein (thrombin, down to 10 nM), and heavy metal ions (Hg^{2+}, down to 5.0 nM) in buffer solutions as well as in real world samples. We have demonstrated that an MB-based biochip is a promising platform for performing rapid, sensitive, cost-effective POC analysis and diagnosis.

ASSOCIATED CONTENT

Supporting Information

Additional experimental data including replicate chip images, ODR/SNR calculations, blocking conditions, mismatch discrimination, and probe sequence optimization. This material is available free of charge via the Internet at http://pubs.acs.org.

AUTHOR INFORMATION

Corresponding Authors

*E-mail: liyc@bnu.edu.cn.
*E-mail: hzyu@sfu.ca.

Notes

The authors declare no competing financial interest.

ACKNOWLEDGMENTS

This work was jointly supported by Beijing Science and Technology New Star Project (2010B021), Scientific Research Foundation for Returned Scholars of Ministry of Education of China, the National Natural Science Foundation of China (NSFC, 21003012, 21273020, 61174010, and 21233003 (the State Key Program)), Fundamental Research Funds for the Central Universities in China (2009SAT-7), and the Natural Science and Engineering Research Council (NSERC) of Canada.

REFERENCES

(1) Soper, S. A.; Brown, K.; Ellington, A.; Frazier, B.; Garcia-Manero, G.; Gau, V.; Gutman, S. I.; Hayes, D. F.; Korte, B.; Landers, J. L.; Larson, D.; Ligler, F.; Majumdar, A.; Mascini, M.; Nolte, D.; Rosenzweig, Z.; Wang, J.; Wilson, D. Point-of-Care Biosensor Systems for Cancer Diagnostics/Prognostics. *Biosens. Bioelectron.* **2006**, *21*, 1932−1942.

(2) Do, J.; Lee, S.; Han, J.; Kai, J. H.; Hong, C. C.; Gao, C.; Nevin, J. H.; Beaucage, G.; Ahn, C. H. Development of Functional Lab-on-a-Chip on Polymer for Point-of-Care Testing of Metabolic Parameters. *Lab Chip* **2008**, *8*, 2113−2120.

(3) Sia, S. K.; Kricka, L. J. Lab on Paper. *Lab Chip* **2008**, *8*, 1988−1991.

(4) Montagnana, M.; Caputo, M.; Giavarina, D.; Lippi, G. Overview on Self-monitoring of Blood Glucose. *Clin. Chim. Acta* **2009**, *402*, 7−13.

(5) Kim, D.; Daniel, W. L.; Mirkin, C. A. Microarray-based Multiplexed Scanometric Immunoassay for Protein Cancer Markers Using Gold Nanoparticle Probes. *Anal. Chem.* **2009**, *81*, 9183−9187.

(6) Ho, C. K.; Robinson, A.; Miller, D. R.; Davis, M. J. Overview of Sensors and Needs for Environmental Monitoring. *Sensors* **2005**, *5*, 4−37.

(7) Kim, P.; Albarella, J. D.; Carey, J. R.; Placek, M. J.; Sen, A.; Wittrig, A. E.; McNamara, W. B., III Towards the Development of a Portable Device for the Monitoring of Gaseous Toxic Industrial Chemicals based on a Chemical Sensor Array. *Sens. Actuator, B* **2008**, *134*, 307−312.

(8) Jiang, A.; Zou, Z.; Lee, K. K.; Ahn, C. H.; Bishop, P. L. State-of-the-Art Lab Chip Sensors for Environmental Water Monitoring. *Meas. Sci. Technol.* **2011**, *22*, 032001.

(9) McGrath, T. F.; Elliott, C. T.; Fodey, T. L. Biosensors for the Analysis of Microbiological and Chemical Contaminants in Food. *Anal. Bioanal. Chem.* **2012**, *403*, 75−92.

(10) Sharma, H.; Mutharasan, R. Review of Biosensors for Foodborne Pathogens and Toxins. *Sens. Actuators B* **2013**, *183*, 535−549.

(11) Chua, A. L.; Yean, C. Y.; Ravichandran, M. A Rapid DNA Biosensor for the Molecular Diagnosis of Infectious Disease. *Biosens. Bioeletron.* **2011**, *26*, 3825−3831.

(12) Hanafiah, K. M.; Garcia, M.; Anderson, D. Point-of-Care Testing and the Control of Infectious Diseases. *Biomarkers Med.* **2013**, *7*, 333−347.

(13) Han, A.; Dufva, M.; Belleville, E.; Christensen, C. B. V. Detection of Analyte Binding to Microarrays Using Gold Nanoparticle Labels and a Desktop Scanner. *Lab Chip* **2003**, *3*, 329−332.

(14) Li, Y.; Ou, L. M. L.; Yu, H.-Z. Digitized Molecular Diagnostics: Reading Disk-Based Bioassays with Standard Computer Drives. *Anal. Chem.* **2008**, *80*, 8216−8223.

(15) Xiang, Y.; Lu, Y. Using Personal Glucose Meters and Functional DNA Sensors to Quantify a Variety of Analytical Targets. *Nat. Chem.* **2011**, *3*, 697−703.

(16) Torabi, S.-F.; Lu, Y. Small-molecule Diagnostics Based on Functional DNA Nanotechnology: a Dipstick Test for Mercury. *Faraday Discuss.* **2011**, *149*, 125−135.

(17) Shen, L.; Hagen, J. A.; Papautsky, I. Point-of-Care Colorimetric Detection with a Smartphone. *Lab Chip* **2012**, *12*, 4240−4243.

(18) Wen, J.; Shi, X. L.; He, Y. N.; Zhou, J. J.; Li, Y. C. Novel Plastic Biochips for Colorimetric Detection of Biomolecules. *Anal. Bioanal. Chem.* **2012**, *404*, 1935−1944.

(19) Alexandre, I.; Hamels, S.; Dufour, S.; Collet, J.; Zammatteo, N.; De Longueville, F.; Gala, J. L.; Remacle, J. Colorimetric Silver Detection of DNA Microarrays. *Anal. Biochem.* **2001**, *295*, 1−8.

(20) Niu, Y. J.; Zhao, Y. J.; Fan, A. P. Conformational Switching Immobilized Hairpin DNA Probes Following Subsequent Expanding of Gold Nanoparticles Enables Visual Detecting Sequence-Specific DNA. *Anal. Chem.* **2011**, *83*, 7500−7506.

(21) Wang, Y. L.; Li, D.; Ren, W.; Liu, Z. J.; Dong, S. J.; Wang, E. K. Ultrasensitive Colorimetric Detection of Protein by Aptamer-Au Nanoparticles Conjugates Based on a Dot-Blot Assay. *Chem. Commun.* **2008**, 2520−2522.

(22) Zhao, W. A.; Ali, M. M.; Aguirre, S. D.; Brook, M. A.; Li, Y. F. Paper-based Bioassays Using Gold Nanoparticle Colorimetric Probes. *Anal. Chem.* **2008**, *80*, 8431−8437.

(23) Xu, H.; Mao, X.; Zeng, Q. X.; Wang, S. F.; Kawde, A. N.; Liu, G. D. Aptamer-Functionalized Gold Nanoparticles as Probes in a Dry-Reagent Strip Biosensor for Protein Analysis. *Anal. Chem.* **2009**, *81*, 669−675.

(24) Cheng, W.; Chen, Y. L.; Yan, F.; Ding, L.; Ding, S. J.; Ju, H. X.; Yin, Y. B. Ultrasensitive Scanometric Strategy for Detection of Matrix Metalloproteinases Using a Histidine Tagged Peptide−Au Nanoparticle Probe. *Chem. Commun.* **2011**, *47*, 2877−2879.

(25) Wang, W.; Wu, W. Y.; Zhong, X. Q.; Wang, W.; Miao, Q.; Zhu, J. J. Aptamer-based PDMS−Gold Nanoparticle Composite as a Platform for Visual Detection of Biomolecules with Silver Enhancement. *Biosens. Bioelectron.* **2011**, *26*, 3110−3114.

(26) Liu, J. W.; Mazumdar, D.; Lu, Y. A simple and Sensitive "Dipstick" Test in Serum Based on Lateral Flow Separation of Aptamer-Linked Nanostructures. *Angew. Chem., Int. Ed.* **2006**, *45*, 7955−7959.

(27) Lee, J. S.; Mirkin, C. A. Chip-based Scanometric Deetection of Mercuric Ion Using DNA-functionalized Gold Nanoparticles. *Anal. Chem.* **2008**, *80*, 6805−6808.

(28) Mazumdar, D.; Liu, J. W.; Lu, G.; Zhou, J. Z.; Lu, Y. Easy-to-Use Dipstick Tests for Detection of Lead in Paints Using Non-cross-linked Gold Nanoparticle-DNAzyme Conjugates. *Chem. Commun.* **2010**, *46*, 1416−1418.

(29) Tyagi, S.; Kramer, F. R. Molecular Beacons: Probes that Fluoresce upon Hybridization. *Nat. Biotechnol.* **1996**, *14*, 303−308.

(30) Tan, W. H.; Fang, X. H.; Li, J.; Liu, X. Molecular Beacons: A Novel DNA Probe for Nucleic Acid and Protein Studies. *Chem.—Eur. J.* **2000**, *6*, 1107−1111.

(31) Li, J.; Geyer, R.; Tan, W. Using Molecular Beacons as a Sensitive Fluorescence Assay for Enzymatic Cleavage of Single-Stranded DNA. *Nucl. Acids Res.* **2000**, *28*, 1−5.

(32) Tang, Z.; Wang, K.; Tan, W.; Li, J.; Liu, L.; Guo, Q.; Meng, X.; Ma, C.; Huang, S. Real-time Monitoring of Nucleic Acid Ligation in Homogenous Solutions Using Molecular Beacons. *Nucl. Acids Res.* **2003**, *31*, e148.

(33) Fang, X.; Liu, X.; Schuster, S.; Tan, W. Designing a Novel Molecular Beacon for Surface-immobilized DNA Hybridization Studies. *J. Am. Chem. Soc.* **1999**, *121*, 2921−2922.

(34) Du, H.; Disney, M. D.; Miller, B. L.; Krauss, T. D. Hybridization-based Unquenching of DNA Hairpins on Au Surfaces: Prototypical "Molecular Beacon" Biosensors. *J. Am. Chem. Soc.* **2003**, *125*, 4012−4013.

(35) Yao, G.; Tan, W. Molecular Beacon-based Array for Sensitive DNA Analysis. *Anal. Biochem.* **2004**, *331*, 216−223.

(36) Chang, H. X.; Tang, L. H.; Wang, Y.; Jiang, J. H.; Li, J. H. Graphene Fluorescence Resonance Energy Transfer Aptasensor for the Thrombin Detection. *Anal. Chem.* **2010**, *82*, 2341−2346.

(37) Zuo, P.; Li, X. J.; Dominguez, D. C.; Ye, B. C. A PDMS/Paper/Glass Hybrid Microfluidic Biochip Integrated with Aptamer-Functionalized Graphene Oxide Nano-Biosensors for One-step Multiplexed Pathogen Detection. *Lab Chip* **2013**, *13*, 3921−3928.

(38) Fan, C.; Plaxco, K. W.; Heeger, A. J. Electrochemical Interrogation of Conformational Changes as a Reagentless Method for the Sequence-Specific Detection of DNA. *Proc. Natl. Acad. Sci. U.S.A.* **2003**, *100*, 9134−9137.

(39) Lu, Y.; Li, X.; Zhang, L.; Yu, P.; Su, L.; Mao, L. Aptamer-Based Electrochemical Sensors with Aptamer-Complementary DNA Oligonucleotides as Probe. *Anal. Chem.* **2008**, *80*, 1883−1890.

(40) Li, D.; Song, S.; Fan, C. Target-Responsive Structural Switching for Nucleic Acid-based Sensors. *Acc. Chem. Res.* **2010**, *43*, 631−641.

(41) Liu, G.; Wan, Y.; Gau, V.; Zhang, J.; Wang, L.; Song, S.; Fan, C. An Enzyme-based E-DNA Sensor for Sequence-specific Detection of Femtomolar DNA Targets. *J. Am. Chem. Soc.* **2008**, *130*, 6820−6825.

(42) Mao, X.; Jiang, J. H.; Xu, X. M.; Chu, X.; Luo, Y.; Shen, G. L.; Yu, R. Q. Enzymatic Amplification Detection of DNA Based on "Molecular Beacon" Biosensors. *Biosen. Bioelectron.* **2008**, *23*, 1555−1561.
(43) Li, J.; Fang, X.; Schuster, S.; Tan, W. Molecular Beacons: a Novel Approach to Detect Protein-DNA Interactions. *Angew. Chem., Int. Ed.* **2000**, *39*, 1049−1052.
(44) Heyduk, T.; Heyduk, E. Molecular Beacons for Detecting DNA Binding Proteins. *Nat. Biotechnol.* **2002**, *20*, 171−176.
(45) Li, J. J.; Fang, X.; Tan, W. Molecular Aptamer Beacons for Real-time Protein Recognition. *Biochem. Biophys. Res. Commun.* **2002**, *292*, 31−40.
(46) Skoog, D. A.; Holler, F. J.; Crouch, S. R. *Principles of Instrumental Analysis*, 6th ed.; Saunders Publishing: New York, 2006; Chapter 5, pp 110−111.
(47) Bockisch, B.; Grunwald, T.; Spillner, E.; Bredehorst, R. Immobilized Stem−Loop Structured Probes as Conformational Switches for Enzymatic Detection of Microbial 16S rRNA. *Nucl. Acids Res.* **2005**, *33*, e101.
(48) Situma, C.; Moehring, A. J.; Noor, M. A. F.; Soper, S. A. Immobilized Molecular Beacons: A New Strategy using UV-activated Poly(methyl methacrylate) Surfaces to Provide Large Fluorescence Sensitivities for Reporting on Molecular Association Events. *Anal. Biochem.* **2007**, *363*, 35−45.
(49) Huang, C. J.; Stakenborg, T.; Cheng, Y.; Colle, F.; Steylaerts, T.; Jans, K.; Dorpe, P. V.; Lagae, L. Label-free Genosensor Based on Immobilized DNA Hairpins on Gold Surface. *Biosens. Bioelectron.* **2011**, *26*, 3121−3126.
(50) Du, H.; Strohsahl, C.; Camera, J.; Miller, B.; Krauss, T. Sensitivity and Specificity of Metal Surface-Immobilized "Molecular Beacon" Biosensors. *J. Am. Chem. Soc.* **2005**, *127*, 7932−7940.
(51) Peterson, A. W.; Heatonand, R. J.; Georgiadis, R. M. The Effect of Surface Probe Density on DNA Hybridization. *Nucl. Acids. Res.* **2001**, *29*, 5163−5168.
(52) Wang, J. Survey and Summary: from DNA Biosensors to Gene Chips. *Nucl. Acids Res.* **2000**, *28*, 3011−3016.
(53) Sassolas, A.; Leca-Bouvier, B. D.; Blum, L. J. DNA Biosensors and Microarrays. *Chem. Rev.* **2008**, *108*, 109−139.
(54) Gupta, S.; Huda, S.; Kilpatrick, P. K.; Velev, O. D. Characterization and Optimization of Gold Nanoparticle-based Silver-Enhanced Immunoassays. *Anal. Chem.* **2007**, *79*, 3810−3820.
(55) Hernández-Rodríguez, N. A.; Correa, E.; Contreras-Paredes, A. Thrombin: A New Useful Factor in the Early Diagnosis of Pulmonary Metastasis. *Rev. Inst. Nal. Cancerol.* **1997**, *43*, 65−75.
(56) Huang, Y. C.; Ge, B.; Sen, D.; Yu, H.-Z. Immobilized DNA Switches as Electronic Sensors for Picomolar Detection of Plasma Proteins. *J. Am. Chem. Soc.* **2008**, *130*, 8023−8029.
(57) Xiao, Y.; Lubin, A. A.; Heeger, A. J.; Plaxco, K. W. Label-free Electronic Detection of Thrombin in Blood Serum by Using an Aptamer-based Sensor. *Angew. Chem., Int. Ed.* **2005**, *117*, 5592−5595.
(58) Chen, C. K.; Huang, C. C.; Chang, H. T. Label-free Colorimetric Detection of Picomolar Thrombin in Blood Plasma Using a Gold Nanoparticle-Based Assay. *Biosens. Bioelectron.* **2010**, *25*, 1922−1927.
(59) Shuman, M. A.; Majerus, P. W. The Measurement of Thrombin in Clotting Blood by Radioimmunoassay. *J. Clin. Invest.* **1976**, *58*, 1249−1258.
(60) Jiang, B. Y.; Wang, M.; Li, C.; Xie, J. Q. Label-free and Amplified Aptasensor for Thrombin Detection Based on Background Reduction and Direct Electron Transfer of Hemin. *Biosen. Bioelectron.* **2013**, *43*, 289−292.
(61) Eisler, R. Mercury Hazards from Gold Mining to Humans, Plants, and Animals. *Environ. Geochem. Health* **2003**, *25*, 325−345.
(62) Wang, Q. R.; Kim, D.; Dionysiou, D. D.; Sorial, G. A.; Timberlake, D. Sources and Remediation for Mercury Contamination in Aquatic Systems - A Literature Review. *Environ. Pollut.* **2004**, *131*, 323−336.
(63) Ono, A.; Togashi, H. Highly Selective Oligonucleotide-Based Sensor for Mercury (II) in Aqueous Solutions. *Angew. Chem., Int. Ed.* **2004**, *43*, 4300−4302.
(64) Chiang, C. K.; Hu ang, C. C.; Liu, C. W.; Chang, H. T. Oligonucleotide-based Fluorescence Probe for Sensitive and Selective Detection of Mercury (II) in Aqueous Solution. *Anal. Chem.* **2008**, *80*, 3716−3721.
(65) Du, J.; Liu, M. Y.; Lou, X. H.; Zhao, T.; Wang, Z.; Xue, Y.; Zhao, J. L.; Xu, Y. S. Highly Sensitive and Selective Chip-based Fluorescent Sensor for Mercuric Ion: Development and Comparison of Turn-on and Turn-off Systems. *Anal. Chem.* **2012**, *84*, 8060−8066.
(66) World Health Organization (WHO). *Guidelines for Drinking-Water Quality*, 3rd ed; World Health Organization: Geneva, Switzerland; Vol. *1*, 2004.